



Predicting organic floc transport dynamics in shallow aquatic ecosystems: Insights from the field, the laboratory, and numerical modeling

Laurel G. Larsen,^{1,2} Judson W. Harvey,² Gregory B. Noe,² and John P. Crimaldi¹

Received 13 June 2008; revised 10 September 2008; accepted 15 October 2008; published 14 January 2009.

[1] Transport of particulate organic material can impact watershed sediment and nutrient budgets and can alter the geomorphologic evolution of shallow aquatic environments. Prediction of organic aggregate (“floc”) transport in these environments requires knowledge of how hydraulics and biota affect the entrainment, settling, and aggregation of particles. This study evaluated the aggregation and field transport dynamics of organic floc from a low-gradient floodplain wetland with flow-parallel ridges and sloughs in the Florida Everglades. Floc dynamics were evaluated in a rotating annular flume and in situ in the field. Under present managed conditions in the Everglades, floc is not entrained by mean flows but is suspended via biological production in the water column and bioturbation. Aggregation was a significant process affecting Everglades floc at high flume flow velocities (7.0 cm s^{-1}) and during recovery from high flow; disaggregation was not significant for the tested flows. During moderate flows when floc dynamics are hydrodynamically controlled, it is possible to model floc transport using a single “operative floc diameter” that accurately predicts fluxes downstream and to the bed. In contrast, during high flows and recovery from high flows, aggregation dynamics should be simulated. When entrained by flow in open-water sloughs, Everglades floc will be transported downstream in multiple deposition and reentrainment events but will undergo net settling when transported onto ridges of emergent vegetation. We hypothesize that net transport of material from open to vegetated areas during high flows is critical for forming and maintaining distinctive topographic patterning in the Everglades and other low-gradient floodplains.

Citation: Larsen, L. G., J. W. Harvey, G. B. Noe, and J. P. Crimaldi (2009), Predicting organic floc transport dynamics in shallow aquatic ecosystems: Insights from the field, the laboratory, and numerical modeling, *Water Resour. Res.*, 45, W01411, doi:10.1029/2008WR007221.

1. Introduction

[2] Predicting the transport of particulate matter in floodplains, wetlands, and slowly flowing streams is often necessary in planning wastewater treatment wetlands, restoration projects, or in determining total maximum daily loads (TMDLs). However, transport predictions are complicated by the tendency of particulate matter to form aggregates, or “flocs,” which may be largely organic. Because of the dynamics of aggregation and disaggregation, and the variable porosity, internal structure, and shape of flocs, floc transport differs substantially from that of the constituent unflocculated material [Walling and Moorehead, 1989; Droppo, 2003; 2004]. Although the transport of inorganic floc is fairly well understood [Lick et al., 1992; Sterling et al., 2005], highly organic floc (hereafter referred to as simply “organic floc”), common in wetlands, has been

less studied. Because of structural differences between organic and inorganic floc (e.g., differences in intraparticle and interparticle cohesion and in the composition and availability of biologically produced exopolymeric substances, or “EPS”), a greater understanding of the dynamics of organic floc is needed to improve the prediction of its transport.

[3] Wetland and floodplain environments pose particular challenges for the prediction of floc transport because of their hydraulics. In contrast to the turbulent flows present in rivers, estuaries, and on the near-bed continental shelf, wetland flows are typically laminar to transitional [Leonard and Luther, 1995; Christiansen et al., 2000; Harvey et al., 2005]. Thus, while turbulence regulates floc size distributions and aggregation-disaggregation processes in the latter environments [Spicer and Pratsinis, 1996; Hill et al., 2001], entrainment/settling fluxes may exert the dominant control over suspended floc size distributions in low-shear environments. Also, while limited, aggregation by turbulent mixing may be more significant than disaggregation in wetland and floodplain environments.

[4] This study is the second in a sequence of experiments designed to improve predictions of organic floc transport in wetlands and shallow, slowly flowing floodplains such as

¹Department of Civil, Environmental, and Architectural Engineering, University of Colorado, Boulder, Colorado, USA.

²U.S. Geological Survey, Reston, Virginia, USA.

the Florida Everglades. In the first study [Larsen *et al.*, 2009], we performed entrainment and settling experiments on Everglades floc, with the finding that this highly organic floc was entrained at lower bed shear stresses (1.0×10^{-2} Pa) than less organic floc and settled more slowly. Morphodynamic differences between floc from sites within the Everglades with different periphyton abundances were small compared to differences between Everglades floc and inorganic floc. In this study we experimentally analyze aggregation dynamics and apply the findings from the present experiment and those of Larsen *et al.* [2009] to numerical models of organic floc transport in wetlands and other slowly flowing shallow aquatic environments. On the basis of these experiments and on a comparison of suspended floc characteristics predicted from laboratory and numerical experiments to those observed in situ, we develop a conceptual model of floc transport in the ridge and slough landscape of the Everglades. To develop the conceptual model and improve predictive numerical modeling of organic floc transport, our experimental and numerical objectives were (1) to determine the flow conditions within the expected range of high flows in the Everglades in which floc aggregation and/or disaggregation becomes significant, (2) to evaluate mechanisms of organic floc aggregation-disaggregation and effects on floc size distributions and fractal dimensions on rising and falling limbs of flow pulses, (3) to evaluate the role of flow-driven entrainment and advection of floc relative to biological production and entrainment of particles in the present-day managed Everglades, and (4) to numerically determine a single operative floc diameter that minimizes error in settling fluxes and downstream transport fluxes and that can be used in simplified models of organic floc transport instead of tracking multiple size classes of floc.

[5] The specific application of this work is to gain a greater understanding of how floc transport dynamics influence the evolution of topography and vegetation patterning in the Everglades. The ridge and slough landscape is a patterned peatland that promotes heterogeneity in vegetation communities and relatively high biodiversity of fish and wildlife [National Research Council, 2003]. For 2700 years, a landscape patterned by elongated (300–1000 m), elevated (60–90 cm historically, 15–20 cm presently) ridges of peat and deeper, open water sloughs (140–360 m wide) aligned parallel to the direction of flow [National Research Council, 2003; Wu *et al.*, 2006] persisted in dynamic equilibrium with the climate [Willard *et al.*, 2001; Bernhardt *et al.*, 2004]. Ridges sustained dense stands of *Cladium jamaicense* (sawgrass), while sloughs were populated by a more diverse vegetation assemblage, dominated by floating mats of *Utricularia* spp. (bladderwort), floating and epiphytic periphyton, *Nymphaea odorata* (water lily), *Nymphoides aquatica* (bleeding heart) and emergent *Eleocharis* spp. (spikerush) [Gunderson and Loftus, 1993; Gunderson, 1994; Lodge, 1994]. Relatively well preserved portions of the ridge and slough landscape persist, but more than 25% of the landscape has deteriorated over the past century, undergoing topographic flattening and conversion of coexisting ridge and slough vegetation communities to *Cladium* monocultures [Bernhardt *et al.*, 2004; Ogden, 2005]. One hypothesis of landscape degradation links ridge spreading and the loss of slough communities to diminished flows,

caused by impoundment and drainage of the Everglades [National Research Council, 2003; Larsen *et al.*, 2007]. According to this hypothesis, historic flows were sufficient to entrain floc from sloughs and ridge margins and redeposit it within ridge interiors, where it would be incorporated into ridge peat and contribute to the corrugation of the landscape (Figure 1a). However, present-day flows are too low to entrain significant quantities of bed floc [Larsen *et al.*, 2009, Figure 7]. To evaluate whether hindered entrainment of floc has contributed to landscape degradation, improved numerical models that better predict sources, sinks, and transport dynamics of floc are needed.

[6] In the Everglades this information is particularly relevant to implementation of the Comprehensive Everglades Restoration Plan [U.S. Army Corps of Engineers, 1999]. Part of this plan will remove levees and canals that impede flow through Everglades marshes with a goal of restoring ridge and slough topography. Establishment of a target flow velocity that redistributes floc and prediction of landscape restoration timescales will be possible with an improved knowledge of floc transport dynamics and incorporation of empirical floc transport results into numerical models. In addition, a greater understanding of the interactions between organic floc and flow could inform predictions of carbon export from floodplains and other shallow, organic-rich aquatic ecosystems that are experiencing changes in carbon balance or flow.

[7] Many of the advances in the prediction of organic floc transport presented here are based on the results of laboratory experiments performed on floc collected from the field. Because of structural disruption (i.e., breakup of large flocs, changes in configuration) that occurs in the process of floc collection [Alldredge and Gotschalk, 1988; Eisma *et al.*, 1990; Winterwerp and van Kesteren, 2004] and differences in the biological and chemical composition of the water column and benthos between the field and the laboratory [Grant and Gust, 1987], results of laboratory experiments should be extended to the field with caution. However, through the use of an in situ digital floc camera (DFC) to monitor floc characteristics without structural disruption in laboratory flumes and through comparison of floc characteristics in the laboratory to those in the field, we took measures to both minimize and assess structural disruption to flocs. We therefore view these experiments as a useful first step in predicting the transport of floc under different Everglades restoration scenarios.

2. Site Description

[8] We experimented on floc from two sites within Water Conservation Area (WCA) -3A, which contains the best preserved portion of the ridge and slough landscape. Field experiments were performed at site WCA-3A-5 (26°03'23.7"N, 80°42'19.2"W), a long-term research site established by the U.S. Geological Survey for the purpose of investigating flow and transport dynamics in the Everglades. The site is equipped with observation platforms, three in situ flumes aligned parallel to the flow, and meteorological and hydrological monitoring instrumentation. The DFC was deployed from one of the platforms at this site in November 2006, when the water depth in the slough was 33.5 cm. At this time, the floc bed was not well developed because of the passage of Hurricane Wilma in October 2005, followed by a

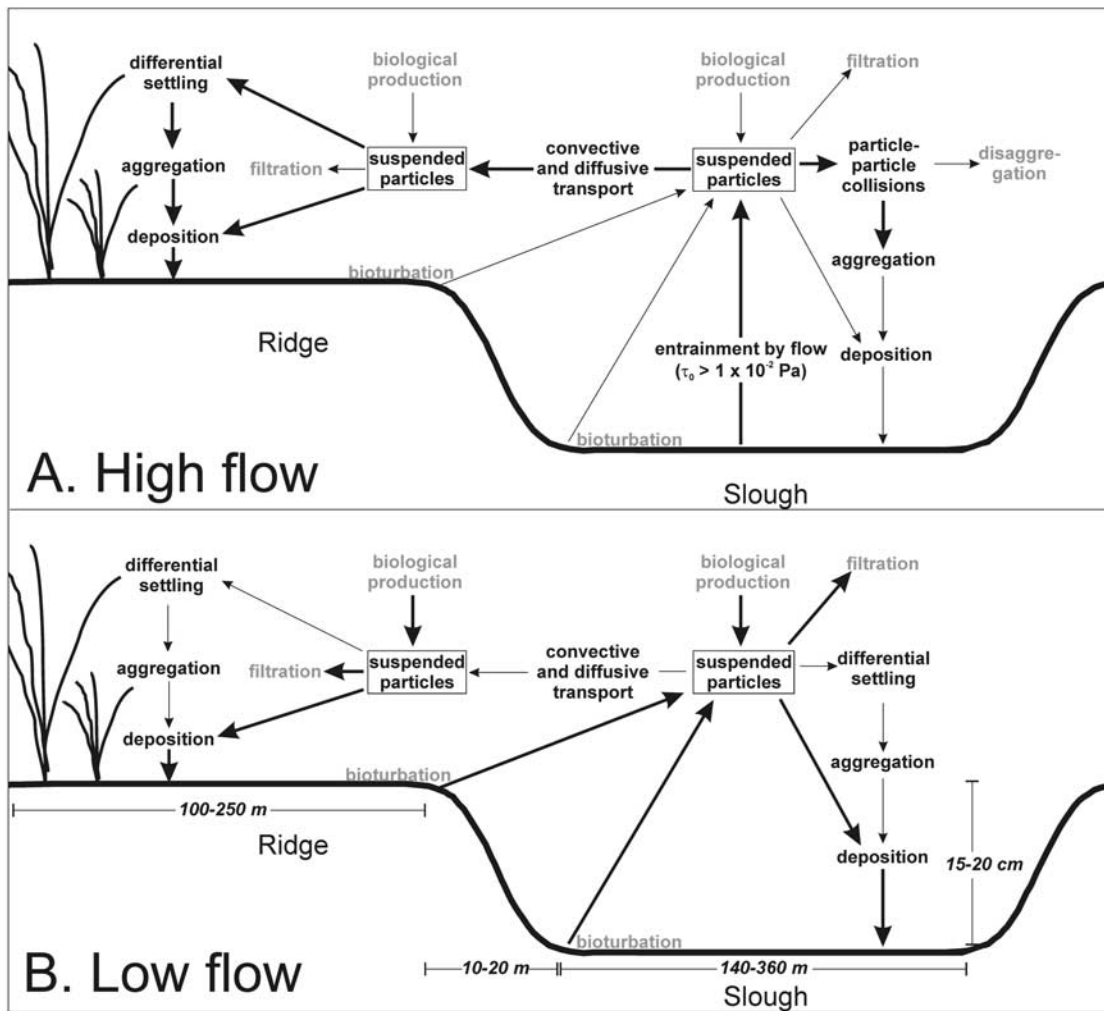


Figure 1. Conceptual model of suspended particle dynamics during (a) high-flow events (associated with a mean bed shear stress above the floc entrainment threshold) and (b) low-flow events in a cross section of the Everglades ridge and slough landscape. Note that the dominant flow direction is orthogonal to the page and that the topography is not to scale. Thick arrows denote dominant transport processes; thin arrows denote less important processes. Differential settling and particle-particle collisions are the processes most directly associated with aggregation of particulate matter to form floc. Gray text describes processes that are beyond the scope of our experimental analysis. Some additional processes affecting suspended particle concentration and ridge and slough landscape evolution are not shown on the diagram, including the size sorting of settling flocs along the ridge-slough transition, biological consumption or decomposition of suspended flocs, resuspension of incompletely deposited flocs (section 4.1), entrainment of epiphyton particles attached to vegetation stems, and photodissolution [Mayer *et al.*, 2006]. Figure 1b also depicts present-day dimensions of landscape cross sections [Wu *et al.*, 2006].

complete drydown in May–July 2006, in which the water table dropped beneath the surface of the peat and the floc layer was incorporated into the peat and/or mineralized. Hurricane Wilma also eliminated the highly productive floating mats of *Utricularia* and periphyton, which might play a substantial role in floc and suspended particle formation [Noe *et al.*, 2007].

[9] Flocculated surface sediment for the aggregation flume experiment was collected from another site in WCA-3A that was more representative of typical conditions in the historic Everglades. In contrast to WCA-3A-5, the “*Utricularia* site,” (26°01′17.9″N, 80°34′45.5″W), main-

tained surface water during the summer of 2006, and floc, *Utricularia*, and periphyton were abundant.

3. Methods

3.1. Experiments

3.1.1. Floc Collection for Laboratory Flume Experiments

[10] As described by Larsen *et al.* [2009], we collected and concentrated flocculated surface sediment from the Everglades using a modified wet/dry shop vacuum. This concentrated sediment was shipped in carboys on ice to the

Table 1. Summary of Flume Experiment Settings and Mean Floc Concentrations

Depth-Averaged Velocity (cm s ⁻¹)	Mean Steady State Floc Concentration					
	Lower Point		Middle Point		Upper Point	
	Mass Concentration (mg L ⁻¹)	Volume Concentration (μL L ⁻¹)	Mass Concentration (mg L ⁻¹)	Volume Concentration (μL L ⁻¹)	Mass Concentration (mg L ⁻¹)	Volume Concentration (μL L ⁻¹)
2.5	0.048	1.5	0.045	3.3	0.031	0.50
4.0	0.23	7.2	0.033	0.81	0.096	3.3
7.0	20	760	13	500	12	400
4.0	2.9	77	1.8	46	1.9	43
2.5	0.31	6.5	0.18	3.4	0.22	3.7

laboratory, refrigerated upon arrival, and used in the aggregation flume experiments within 1.5 weeks of collection. To judge the likeness between the collected laboratory aggregates and floc in the field, we determined the bulk density of both floc bed populations in quiescent water by collecting 4.8 cm diameter cores containing the flocculated sediment, a small amount of underlying substratum (more compacted peat), and enough of the overlying surface water to allow the floc within the cores to settle to a thickness that could be visually determined through the clear core sleeve. We then decanted and freeze dried the floc to determine its dry mass.

3.1.2. DFC Configuration

[11] Floc was imaged in situ in the laboratory flume and in the field using a silhouette imaging technique with a digital single-lens reflex camera controlled remotely by a laptop computer [Larsen *et al.*, 2009]. In the laboratory, the camera was placed outside the clear flume wall, facing a synchronized light source in a watertight housing on the inside of the flume. In the field, both the light source and the camera were deployed in watertight housings. Image resolution in both configurations was 14.50 μm per pixel, with a 4.13 cm × 6.22 cm field of view and a 2.5 cm depth of field. Since flocs were defined by a minimum of three pixels, the DFC resolved flocs with a minimum size of 43.50 μm.

3.1.3. Aggregation-Disaggregation Experiments

[12] Aggregation-disaggregation experiments took place in a rotating annular flume at the Institute of Marine and Coastal Sciences, Rutgers University. The annular flume is well suited for aggregation experiments because of its small bed area (which can be completely covered with sediment) and its ability to recirculate floc without pumps (which cause structural disruption to aggregates). Rotation of the flume lid drives the flow, permitting entrained flocs to circulate without structural disruption, whereas counterrotation of the sidewalls and the bed minimizes centrifugal effects and produces the bed shear stresses that are nearly uniform across the radius of the flume [Krishnappan, 1991, 1993; Petersen and Krishnappan, 1994].

[13] Experiments occurred at three different mean velocities that exceeded the 90th percentile for present-day flows in the Everglades [Harvey *et al.*, 2008]: 2.5 cm s⁻¹, 4.0 cm s⁻¹, and 7.0 cm s⁻¹. For each experiment, the water depth was 45 cm, and the homogeneous floc bed was allowed to settle for 24 h prior to experimentation. In all runs, the 3 cm thickness of the floc bed was sufficient to prevent complete erosion. After experimental runs (but with all instruments and floc present in the flume), we used a two-component Dantec laser Doppler velocimeter (LDV) to acquire centrally located velocity profiles at 20 logarithmically spaced points

(see auxiliary material), each of which was sampled for 17 min to ensure convergence of flow statistics [Larsen, 2008].¹ Abbreviated velocity profiles (8 points) acquired during experimental runs confirmed that the complete profiles were representative of flow during all runs (see auxiliary material).

[14] The DFC was mounted to a profiler outside the flume that was attached to a planar, Plexiglas observation port. A second profiler mounted inside the flume to the top of the observation port supported the flash. For the duration of each experiment, which consisted of five consecutive intervals (Table 1), images were acquired at 0.1 Hz. In the first three intervals (“increasing velocity intervals”), the flow velocity was increased at the start of the run and held constant for 1 h, exceeding the 25 min required to attain an equilibrium suspended floc size distribution at the fastest flow speed. In the last two intervals (“decreasing velocity intervals”), the velocity was initially decreased and then maintained at a constant level for 1.5 h, since disaggregation timescales (maximum of 67 min) exceeded aggregation timescales [Larsen, 2008]. Since it was necessary to stop the flume and raise the lid to change the vertical position of the flash housing, three experiments (each consisting of the aforementioned 5 intervals) were conducted to image floc at three levels: 11.7 cm, 16.2 cm, and 26.7 cm above the bed. Between runs, the floc bed settled for 24 h.

3.1.4. Field Observations

[15] We observed flow velocities and suspended floc size distributions in situ at the WCA-3A-5 field site during a short-term diel experiment on 28–29 November 2006, between 1530 and 1000 local time. The purpose was to compare suspended floc characteristics under the controlled hydraulic conditions of the laboratory to actual floc dynamics in the measured hydraulics of the field and to evaluate whether physical forcing by mean flow or other processes (e.g., thermal overturn, biological processes) exerts the dominant control over suspended sediment dynamics in the Everglades.

[16] Both the DFC and the flash were deployed from an aluminum profiler supported above the water by the sidewalls of an open flume within the ridge-slough transition zone. For most of the monitoring period, the center of the images was 10 cm above the peat bed, and an image was acquired every 10 min (to conserve equipment battery life). Mounted to a profiler attached to the flume 3 m upstream, a Son Tek Acoustic Doppler Velocimeter monitored the ambient flow velocity. Velocity statistics were obtained

¹Auxiliary materials are available in the HTML. doi:10.1029/2008WR007221.

19 cm above the floc bed. Using a thermistor array, we monitored the vertical stratification in surface water temperature throughout the night. When we observed the initiation of thermal overturn, a nightly occurring convective process hypothesized to cause floc entrainment [Schaffranek and Jenter, 2001], we conducted a six-point vertical profile of suspended floc concentrations and water velocity. After slowly raising the instruments to each new profile point, we waited 2 min before resuming data collection to allow disturbed flocs to settle. Flocs generally settling at speeds of between 0.4 and 1 mm s⁻¹ [Larsen et al., 2009] would clear the 4.1 cm–high field of view within this lag time. At each point, images were acquired for 2 min at 1/6 Hz.

3.2. Analysis

3.2.1. General Image Processing

[17] Projected flocs were delineated from image backgrounds by binarization, which first involved subtraction of a dark current image and a background image from each raw gray-scale image. In the laboratory, the background image was averaged from 10 images acquired in quiescent water with no suspended floc. In the field it was not possible to acquire a controlled background image, so a dynamic background that was computed by averaging up to 15 images before and after each image in the sequence was subtracted from the gray-scale image. The semiprocessed images were then binarized by thresholding [Larsen et al., 2009]. Postbinarization, each image was checked by an operator to ensure that lighting conditions had a consistent effect on thresholding, and masks were created to remove bubbles, large nekton (from the field images), and particles that adhered to the imaging equipment. Finally, aggregate equivalent diameter (computed as the diameter of a circle with area equivalent to the area of the digitized floc), perimeter (p), area (A), assumed spherical volume (computed from equivalent diameter), and fractal dimension (D) were computed from the binarized images. Assumed spherical volumes were converted to floc concentration by dividing by a control volume delineated by the imaging hardware and the known camera field of view. In the field the thickness of the control volume was bounded by the vertical faces of the flash and camera housings, whereas in the laboratory flume, the face of the flash housing and the flume wall provided the vertical bounds. Finally, a fractal dimension for projected flocs [de Boer, 1997; Stone and Krishnappan, 2003] was defined by

$$p \sim A^{D/2}. \quad (1)$$

3.2.2. Aggregation-Disaggregation Experiments

[18] An aggregation parameter (a , L μL^{-1}) was determined through a transient, one-dimensional, reactive transport model describing mass transfer in the annular flume experiment. Using the aggregation model of Winterwerp and van Kesteren [2004] to formulate a reaction term that describes the effects of aggregation (third term on the right-hand side below), we derived the relevant transport equation as follows, assuming uniform flow:

$$\frac{\partial C_i}{\partial t} = K \frac{\partial^2 C_i}{\partial z^2} + w_s \frac{\partial C_i}{\partial z} + a\alpha^2 C_i^2 G, \quad (2)$$

where C_i is the volumetric floc concentration in size class i ($\mu\text{L L}^{-1}$), K is turbulent eddy diffusivity ($\text{cm}^2 \text{s}^{-1}$), z is the

vertical coordinate (cm), w_s is the floc settling velocity in size class i (cm s^{-1}), α is a constant of proportionality that converts the concentration within the size class to the total floc concentration, and G is the shear rate parameter (s^{-1}). C_i and α were determined from the annular flume DFC images, while w_s was determined from the companion experiments of Larsen et al. [2009]. Vertical profiles of K were computed from LDV data as described by Larsen et al. [2009]. G , a measure of turbulent shear at the smallest length scales of the flow, was calculated from the equation $G = \sqrt{\varepsilon/\nu}$ [Winterwerp and van Kesteren, 2004], where ν is the kinematic viscosity and ε is the turbulent kinetic energy dissipation rate. We approximated ε using the relation given by Nezu and Nakagawa [1993]

$$\varepsilon \approx \frac{u_*^3(1-z/h)}{\kappa h(z/h)} \quad (3)$$

where h is water depth and κ is the von Karman constant (0.41). Shear velocity, u_* , was estimated as $0.05\langle\bar{u}\rangle$.

[19] The third term on the right-hand side of equation (2) is a reaction term that describes aggregation. If a is negative, floc is lost from size class i via aggregation to form larger flocs. In contrast, positive values of a occur when concentrations of floc in size class i are augmented by aggregation of particles from a different size class. When aggregation occurs, a for smaller size classes is negative, while a for larger size classes is positive. Typically, flocculation models also include a term for disaggregation, $d_1\alpha C_i G^{d_2}$, where d_1 and d_2 are both constants [Winterwerp and van Kesteren, 2004]. However, when we attempted to include a disaggregation term in our model, we could not resolve unique values of the fitting parameters because of an underconstrained system. Since results (section 4.1) indicated a clear dominance of aggregation processes over disaggregation processes, we retained only $a\alpha^2 C_i^2 G$, which served as a net aggregation term.

[20] Boundary conditions for equation (2) are zero flux at the water surface and a flux of ($J_e - w_s C_{i,z\text{min}}$) at the bed, where J_e is entrainment flux ($\text{g cm}^{-2} \text{s}^{-1}$), assumed constant within each size class and each run, and $C_{i,z\text{min}}$ is the floc concentration in the bottom cell of the model domain. Since the configuration of the flume prevented measurement of flow statistics within 3 cm of the bed, J_e was treated as a fitting parameter in the model and numerically optimized from the transport model and the time series of observed suspended floc concentrations.

[21] We used equation (2) to solve for J_e and a in each of the five intervals of the aggregation-disaggregation experiments (Table 1). Predicted concentrations at each DFC image acquisition time were spatially averaged over the range of z coordinates imaged by the DFC at the upper, middle, and lower locations and compared to imaged concentrations. Using a Levenberg-Marquardt algorithm, J_e was fit for each size class at each flume speed to minimize the total error between predicted and observed floc concentrations over all three image locations and all sampling times. We then used the fitted J_e to initialize a second Levenberg-Marquardt procedure in which both J_e and a were adjusted. Since a was fit for each size class independently, this procedure did not ensure conservation of mass across all size classes.

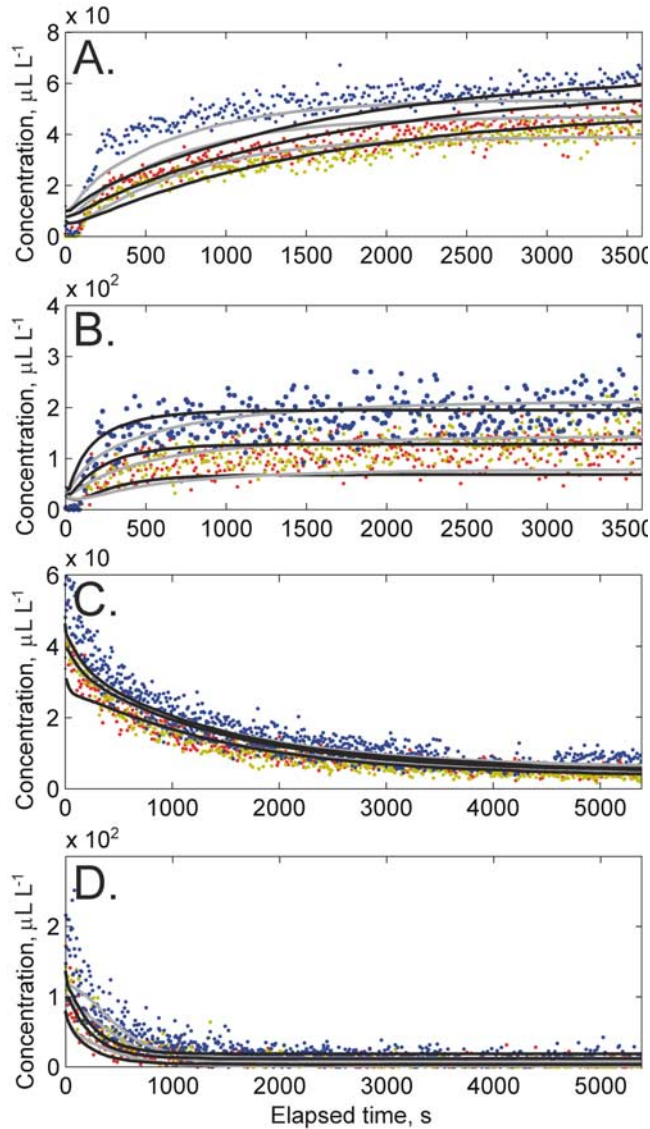


Figure 2. Sample floc transport model results (solid lines) compared with experimental data (points) for annular flume runs. Gray lines are simulation results using the optimized aggregation parameter, and black lines were generated using an aggregation parameter of zero. The blue, yellow, and red points represent data for the lower (11.7 cm above bed), middle (16.2 cm above bed), and upper (26.7 cm above bed) imaging locations, respectively. Shown are (a) 0–250 μm size class, 7 cm s^{-1} flume interval; (b) 500–750 μm size class, 7 cm s^{-1} flume interval; (c) 0–250 μm size class, 4 cm s^{-1} decreasing velocity flume interval; and (d) 500–750 μm size class, 4 cm s^{-1} decreasing velocity flume interval.

[22] Finally, to assess the relative importance of floc aggregation processes, we defined an instantaneous Damköhler number (Da) as the ratio of the settling timescale to the aggregation timescale [Sterling *et al.*, 2005], equivalent to the ratio of the rate of change in C_i due to aggregation to the rate of change in C_i due to settling:

$$\text{Da} = \frac{a\alpha^2 C_i^2 G}{w_s \partial C_i / \partial z}. \quad (4)$$

We preserved signs so that a negative Da occurred when the effect of aggregation countered the net effect of settling. A positive Da occurred for small size classes when aggregation converted small flocs to large flocs, removing them from the small size classes.

4. Results and Discussion

4.1. Aggregation Processes Affecting Organic Floc

[23] The shape of the curve describing suspended floc concentration over time in the annular flume experiments (Figure 2) is informative of floc aggregation dynamics. Following an increase in velocity (Figures 2a and 2b), floc concentrations rise steeply as a result of enhanced entrainment. Later (within 8–17 min in our experiments), suspended floc concentrations stabilize at a steady value that reflects a balance between entrainment, settling, and net aggregation. When aggregation dominates over disaggregation, floc is removed from smaller size classes (decreasing the steady state concentration of these size classes) and added to larger size classes (increasing their steady state concentration).

[24] Since both the entrainment flux and aggregation parameter for each size class in the annular flume are unknown a priori, multiple combinations of entrainment and aggregation can produce the observed steady state concentration. However, unique values of the aggregation parameter a and the size class-specific entrainment flux J_e can be optimized from equation (2) because the aggregation flux, $a\alpha^2 C_i^2 G$, is proportional to the square of floc concentration. For increasing velocity intervals, aggregation is relatively unimportant on the rising limb of the curve, before concentrations are high. The rising limb is therefore dominated by J_e . Its shape enables J_e to be determined uniquely, and a can then be solved from the steady state part of the curve. In contrast, for decreasing velocity intervals (Figures 2c and 2d), the low-concentration, steady state portion of the transient curve is dominated by J_e , while aggregation is only important on the falling limb of the curve. For these intervals, the shape of the falling limb is important in optimization of a , though the statistical confidence in the optimized value is less than that for the increasing velocity intervals because of the relatively short period of time occupied by the falling limb and the decreasing importance of aggregation along this portion of the curve.

[25] Results of parameter optimization for the transport model (equation (2)) showed that aggregation was significant (95% confidence intervals surrounding a did not intercept zero) only for size classes 0–1750 μm of the 7 cm s^{-1} increasing velocity interval and for size classes 0–1500 μm of the 4 cm s^{-1} decreasing velocity interval (Table 2). Only within the 0–250 μm size class was a negative, indicating that these flocs aggregate to form larger flocs. For these experimental runs, our transport model with an a of zero could not reproduce the shape of the sensitive rising and falling limb portions of the transient concentration curves (Figure 2), though for the remaining runs (2.5 cm s^{-1} increasing and decreasing, 4 cm s^{-1} increasing), a reasonable fit was obtained in the absence of an aggregation parameter. Because of aggregation and an increase in J_e during the decreasing velocity intervals (Table 3), equilibrium floc sizes

Table 2. Significant Fitted Values of Floc Aggregation Term a^a

Size Class (μm)	Aggregation Term a With 4 cm s^{-1}	Aggregation Term a With 7 cm s^{-1}
	Decreasing Velocity Interval ($\text{L } \mu\text{L}^{-1} \times 10^{-5}$)	Increasing Velocity Interval ($\text{L } \mu\text{L}^{-1} \times 10^{-5}$)
0–250	-0.6 ± 0.5	-0.7 ± 0.1
250–500	26.6 ± 0.9	1.2 ± 0.3
500–750	25.3 ± 0.7	3.2 ± 0.3
750–1000	15.9 ± 0.4	2.4 ± 0.4
1000–1250	7.8 ± 0.4	1.8 ± 0.1
1250–1500	4.8 ± 0.4	0.6 ± 0.6
1500–1750		0.4 ± 0.2

^aSee equation (2). The aggregation term is significant when its 95% confidence intervals (the given range) do not intercept zero.

were larger in the decreasing velocity intervals than in the corresponding increasing velocity intervals (Figure 3a). Although a was not statistically significant for large size classes (1750–3500 μm) within the 7 cm s^{-1} increasing velocity and 4 cm s^{-1} decreasing velocity intervals, it is likely that aggregation augmented these size classes as well, though the relative rarity of these large flocs resulted in an ill-constrained transport model. Additional noise in the model fit to observed concentration curves could have resulted from changes in mean bed floc size between runs, sorting of the floc bed during previous deposition events [Lau et al., 2001], and changes in sediment stability as a result of previous erosion/deposition cycles [Droppo et al., 2001].

[26] While floc aggregation was significant during both the 7 cm s^{-1} increasing velocity interval and 4 cm s^{-1} decreasing velocity interval, the large difference in the optimized value of a for each size class between these two runs (Table 2), together with the difference in the steady state fractal dimension D across intervals (Figure 3b), suggests that aggregation occurred via different mechanisms [Winterwerp and van Kesteren, 2004]. A decrease in D (e.g., from the 4 cm s^{-1} increasing velocity interval to the 7 cm s^{-1} interval) typically indicates the existence of floc shearing [Logan and Wilkinson, 1990; Huang, 1994; Dyer and Manning, 1999], which begins at shear stresses near 0.1 Pa [Hill et al., 2001]. Thus, relatively low values of both D (Figure 3b) and a (Table 2) during the 7 cm s^{-1} run evidence particle-particle collisions that resulted in floc erosion and disaggregation as well as aggregation [Burban et al., 1989; Lick et al., 1992; Spicer and Pratsinis, 1996]. Since in the absence of a disaggregation term, $a\alpha^2 C_i^2 G$ described net aggregation, a would have absorbed the influence of floc disaggregation. In contrast, an increase in

D (e.g., from the 7 cm s^{-1} interval to the 4 cm s^{-1} decreasing velocity interval) often indicates aggregation by differential settling [Huang, 1994; Chen and Eisma, 1995], a process in which rapidly settling large particles intercept and capture more slowly settling small particles [Logan and Wilkinson, 1990; Huang, 1994; Thomas et al., 1999]. During the 4 cm s^{-1} run, a net flux of sediment to the bed occurred, and differential settling may have become the primary mechanism of aggregation, while disaggregation by shear was minimal.

[27] Simulated Damkohler numbers (Figure 4) show that the aggregation flux was most significant relative to the settling flux in high-shear, high-concentration portions of the water column, particularly near the bed, where Da ranged between order 0.1 and order 10. In these locations, both turbulent mixing and differential settling bring particles in contact and cause aggregation. Large aggregation fluxes near the bed during periods of elevated flow will thus enhance sediment deposition in wetlands and slowly flowing floodplains. In contrast, in estuaries and other turbulent environments, net disaggregation in the high-stress region near the bed counters net aggregation in relatively low-

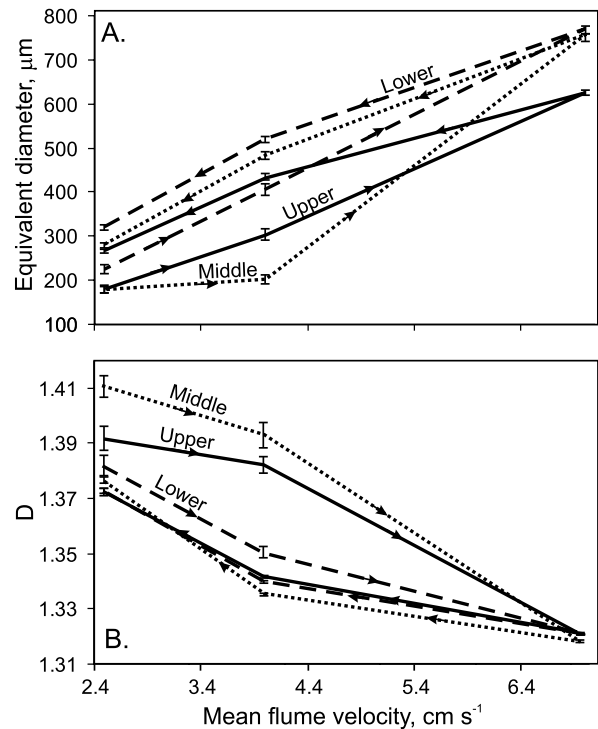


Figure 3. Hysteresis in (a) equivalent diameter and (b) fractal dimension D for the upper, middle, and lower image locations during the annular flume aggregation experiments. Volume-weighted mean equivalent diameter and mean fractal dimension were computed for the steady state portion of the concentration curves after 500 s in the increasing velocity experimental intervals and after 1000 s in the decreasing velocity intervals. Arrows indicate the direction in which equivalent diameter and D progress through the experiment, and error bars are 95% confidence intervals around the mean values.

Table 3. Average Entrainment Flux Across All Size Classes During Annular Flume Runs

Mean Flow Velocity (cm s^{-1})	J_e , Increasing Velocity Interval ($\text{cm}^3 \text{ cm}^{-2} \text{ s}^{-1}$)	J_e , Increasing Velocity Interval ($\text{cm}^3 \text{ cm}^{-2} \text{ s}^{-1}$)
2.5	2.6×10^{-7}	2.9×10^{-6}
4	8.3×10^{-7}	4.1×10^{-6}
7	5.0×10^{-5}	

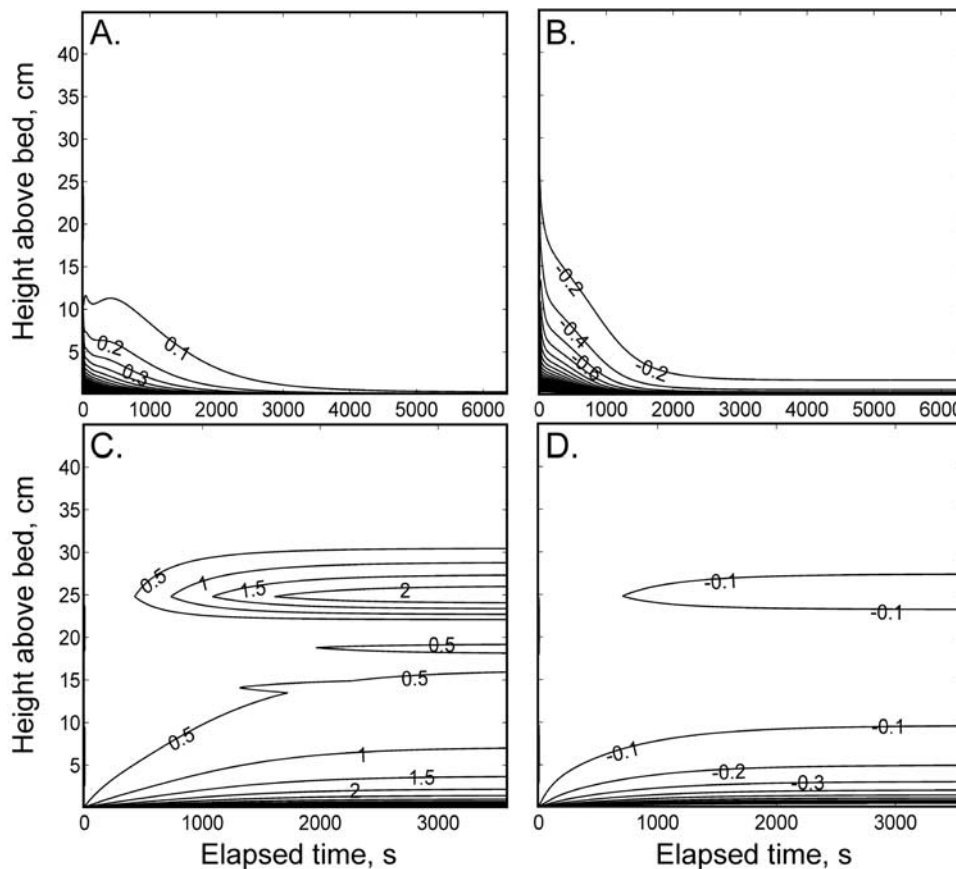


Figure 4. Representative distributions of instantaneous Damkoehler number, comparing floc aggregation rate to floc settling rate, over depth and time in the optimized simulations of the annular flume experiment. Damkoehler numbers for the 4 cm s^{-1} decreasing velocity experimental interval: (a) $0\text{--}250 \mu\text{m}$ size class, 4 cm s^{-1} decreasing velocity interval; (b) $250\text{--}500 \mu\text{m}$ size class, 4 cm s^{-1} decreasing velocity interval; (c) $0\text{--}250 \mu\text{m}$ size class, 7 cm s^{-1} interval; and (d) $250\text{--}500 \mu\text{m}$ size class, 7 cm s^{-1} interval. Distributions of Damkoehler numbers for size classes up to $1500\text{--}1750 \mu\text{m}$ are qualitatively similar to Figures 4b and 4d but with different magnitudes, reflecting differences in the magnitude of aggregation parameter a (Table 2).

stress regions high in the water column and decreases deposition fluxes [Mehta and Partheniades, 1975; Partheniades, 1977].

[28] The laboratory annular flume configuration lacks the biotic composition of the water column in the field and the production of new detrital particles, so experimental results provide a conservative estimate of the aggregation that occurs in the field as a result of turbulent mixing and differential settling [Winterwerp and van Kesteren, 2004]. In the field, aggregation via turbulent mixing and differential settling, particularly near the bed, will therefore be highly significant during periods of elevated flow and recovery from elevated flow.

4.2. Field Deployment of the DFC

[29] Floc observed in situ at site WCA-3A-5 was morphologically similar to the aggregates collected for the annular flume experiments (Figure 3), with a daytime and nighttime mean D of 1.43 ± 0.02 and 1.37 ± 0.01 (error values are 95% confidence intervals), respectively, providing validation for the technique of allowing deposited floc beds to settle in the flume for 24 h prior to experimentation. However, the bulk density of the floc bed in the field, at $1.3 \times 10^{-2} \text{ g cm}^{-3}$ ($N = 1$ core), was slightly higher than the bulk

density of the laboratory floc bed ($8.4 \times 10^{-3} \text{ g cm}^{-3}$, $N = 1$ core), reflecting a small structural difference in floc bed compaction. Mean mass-weighted equivalent diameter over the diel time series was $262 \pm 130 \mu\text{m}$.

[30] During the period of field deployment of the DFC, ADV measurements of flow velocity ranged between 0.24 cm s^{-1} and 0.40 cm s^{-1} , with a mean of 0.33 cm s^{-1} . Instantaneous flow velocities were not significantly correlated with suspended floc concentration ($F_{1,23} = 1.80$, $p = 0.19$, r^2 of linear regression = 0.07) which was more variable, ranging from $9.4 \times 10^{-4} \text{ mg L}^{-1}$ to 0.31 mg L^{-1} , with a mean of 0.061 mg L^{-1} . After sundown (17:29), suspended floc concentrations and mean size exhibited large spikes until around 3:30, when concentrations decreased and remained variably low until a spike around 8:30 (Figure 5). The lack of correlation between flow characteristics and floc concentrations suggest that during the period of monitoring, biological activity such as fecal pellet production or bio-turbation by nocturnal *Palaeomonetes paludosus* (grass shrimp), *Procambarus* spp. (crayfish) or other crustaceans might have had the dominant influence on measured concentrations. We noticed many small and several large crustaceans in our nighttime images, and while we removed

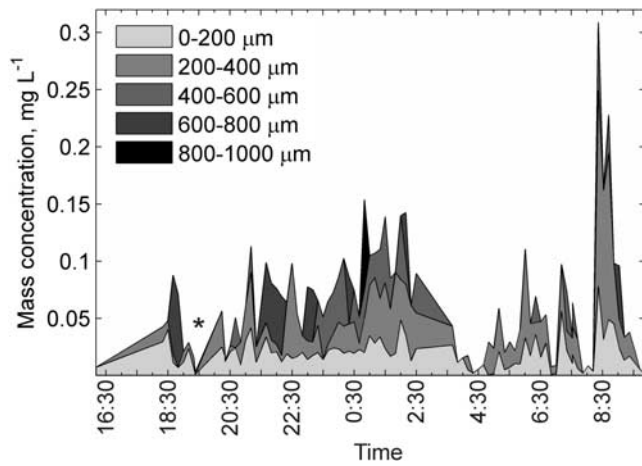


Figure 5. Distribution of floc size class concentrations through the 28–29 November 2006 sampling period at site WCA-3A-5. The asterisk denotes the period during which thermal overturn occurred in the water column.

the most obvious organisms by masking, smaller zooplankton were doubtlessly binarized as floc. Other data sets from WCA-3A-5 show that temporal variation in the concentrations of small particles ($1.25\text{--}250\ \mu\text{m}$) is also likely dominated by biological activity, with spikes in concentration throughout the night and a sustained and significant increase in bacteria-sized particles ($1.44\text{--}2.31\ \mu\text{m}$) that are enriched in microbially bound phosphorus after sunrise [Noe *et al.*, 2008]. We did not observe a sustained daytime increase in floc concentrations, but the 30-min long spike in concentration at 8:30 is consistent with a hypothesis of floc entrainment via bioturbation [National Research Council, 2003] from temporary *Gambusia holbrooki* (mosquito fish) activity, which tends to be highly localized.

[31] Suspended floc concentrations during the period of thermal overturn were among the lowest for the night (Figure 5), which fails to support a hypothesis of enhanced entrainment by turbulence associated with thermal convection [Schaffranek and Jenter, 2001] and may reflect advective delivery of floc to the bed. At points higher than the diel monitoring location (10 cm above bed) during the thermal overturn, floc mass concentrations were nearly equivalent to or lower than concentrations near the bed (not shown). Within the vertical profile, pairwise correlations between concentrations of floc in the different size classes were insignificant (Spearman's ρ , all $p > 0.07$, $N = 6$ depths), supporting a hypothesis of biological rather than fluid mechanical dominance over the floc concentration profiles under present flow conditions. The highest correlate to overall floc concentration at a given level in the water column was concentration of floc within the $200\text{--}400\ \mu\text{m}$ size class (Spearman's $\rho = 0.83$, $p = 0.04$), which encompasses the size range of many zooplankton [Masson *et al.*, 2004] that may not have been excluded by masking.

[32] Suspended floc concentrations observed in the field with the DFC were higher than those observed in a companion racetrack flume entrainment experiment for comparable flow velocities ($7.6 \times 10^{-3} - 1.2 \times 10^{-2}\ \text{mg L}^{-1}$ for velocities of $0.6\text{--}1.4\ \text{cm s}^{-1}$ [Larsen *et al.*, 2009]). The reason is that while concentrations of suspended floc

are governed by physical processes in the laboratory flume, floc concentrations in the field are enhanced by bioturbation and the continual production of new particles (e.g., fecal material, EPS) by biota in the water column (Figure 1). Nevertheless, the concentrations of floc that we measured in suspension in the Everglades ($0.001\text{--}0.3\ \text{mg L}^{-1}$) and also in the laboratory flumes at moderately high velocities ($0.003\text{--}0.3\ \text{mg L}^{-1}$) were substantially lower than concentrations of fine suspended particles ($0.2\text{--}100\ \mu\text{m}$) measured in a study that used sequential filtration to assess particle concentrations in samples collected from across the Everglades ($0.7\text{--}2.7\ \text{mg L}^{-1}$ [Noe *et al.*, 2007]) and over two wet seasons at site WCA-3A-5 (mean = $0.94\ \text{mg L}^{-1}$ [Noe *et al.*, 2008]) under normal flow conditions. Thus, it appears that even during high-flow events, fine particles contribute substantially to the suspended particle load in the Everglades.

4.3. Modeling Wetland Suspended Floc Dynamics

[33] The low shear present within the Everglades and other wetlands and floodplains permits the coexistence of a wide range of floc sizes, settling velocities, and entrainment fluxes. Such variability presents challenges for modeling, often creating the need to simultaneously track multiple size classes of floc [Thomas *et al.*, 1999]. Exchange between size classes via aggregation and disaggregation processes, a change in the dominant mechanism of aggregation between rising and falling limbs of suspended floc concentration curves, and the importance of biological processes present additional modeling challenges. Unfortunately, full mass balance modeling of multiple size classes of suspended floc may be computationally prohibitive in large-scale, coupled models. However, there are reasonable simplifications that can be made to floc transport equations that preserve the essence of the physical dynamics.

[34] We introduce the concept of an “operative floc diameter” (OFD) to use in simplified advection-dispersion equations. The OFD differs from the equivalent diameter used earlier (i.e., the diameter based on digitized floc area). OFD, which can be either lower or higher than the mean equivalent diameter, is the diameter at which settling and entrainment fluxes are equal to actual bed fluxes across all particle size classes at steady state and in which error in the vertically averaged floc concentration is minimized. Because of nonlinearities in vertical profiles of suspended floc concentration, use of the mean equivalent diameter rather than the OFD can introduce large errors in computed fluxes. In a simplified modeling scheme, an overall entrainment flux that is independent of floc size and is a function of bed shear stress and the critical shear stress for floc entrainment [e.g., Larsen *et al.*, 2009] can be used in tandem with a settling velocity determined from the OFD to accurately capture the balance between entrainment and deposition fluxes to the bed and the rate of mass transfer downstream.

[35] To determine the OFD for the Everglades, we employed a logarithmic velocity profile, which approximates flow in sloughs [Harvey *et al.*, 2008]. Steady state suspended sediment concentration profiles in flow with a logarithmic boundary layer velocity profile follow the Rouse equation [Middleton and Southard, 1984]:

$$\frac{C(z)}{C_a} = \left(\frac{z_a}{z}\right)^{\frac{w_s}{\sigma_{TKHS}}}, \quad (5)$$

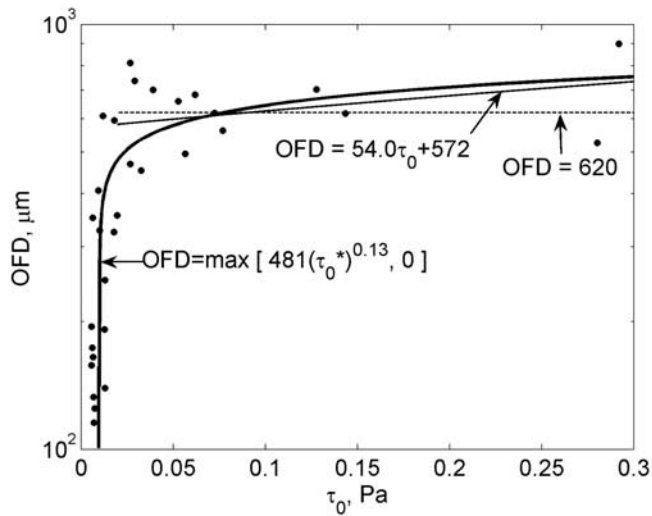


Figure 6. Operative floc diameter (OFD) computed for floc populations in the racetrack flume entrainment experiments at different values of the normalized excess bed shear stress ($\tau_0^* = (\tau_0 - 1.0 \times 10^{-2} \text{ Pa}) / 1.0 \times 10^{-2} \text{ Pa}$). The OFD is that at which errors in vertically averaged floc concentration are minimized and the settling and entrainment fluxes at the bed are exactly equal to those of actual floc with a distribution of equivalent diameters. In this computation, the OFD is based on a logarithmic velocity profile and a steady state floc concentration profile. OFD values computed with data from the racetrack flume experiment for bed shear stresses greater than the entrainment threshold are fit with three regression lines: (1) a power law regression (thick line); (2) a linear regression (thin line); and (3) a constant, equal to the mean value of OFD for bed shear stresses above $2.0 \times 10^{-2} \text{ Pa}$ (dashed line).

where C_a is the concentration at reference location $z = z_a$, σ_T is the turbulent Schmidt number (assumed unity), and u^* is equal to $\sqrt{\tau_0/\rho}$. In this analysis, we assumed that z_a is located just above the bed (0.05 mm in our discretized solution). For each point on a measured floc entrainment curve [Larsen *et al.*, 2009], we set C_{ai} (the value of C_a within each size class i) equal to J_e/w_{si} , which assumes steady state at the bed. Solving equation (5) for size class i and a 40 cm water column and then summing over all size classes, we obtained the total concentration profile at each bed shear stress. Using a Levenburg-Marquardt algorithm, we then selected the single value of w_s that satisfied $C_a = J_e/w_s$ (where J_e is the overall entrainment flux as a function of bed shear stress) and minimized the overall error in depth-averaged floc concentration, computed from the profile in equation (5). Finally, from the calibrated w_s and a regression equation for measured w_s as a function of floc equivalent diameter [Larsen *et al.*, 2009], we determined the OFD.

[36] OFDs were accordingly calculated from 32 runs of a flume entrainment experiment for Everglades floc, reported by Larsen *et al.* [2009]. For each of these runs, use of a single OFD resulted in an error in depth-averaged concentration ranging from 0.01% to 0.2%. The curve of OFD as a function of bed shear stress (Figure 6) increased rapidly with bed shear stress near the entrainment threshold and then increased more slowly with further increases in bed

shear stress. The standard error of a power law regression (147 μm) was slightly worse than the standard error of linear regression (143 μm) on the OFD at bed shear stresses in the asymptotic portion of the curve ($\tau_0 \geq 2.0 \times 10^{-2} \text{ Pa}$), advocating use of the simplest OFD relationship. Although the standard error of linear regression was slightly better than the error (151 μm) of approximating the OFD curve as the mean OFD above bed shear stresses of $2.0 \times 10^{-2} \text{ Pa}$, the slope of the linear regression was insignificant ($t_{df=13} = 1.24$, $p = 0.24$). Thus, in modeling suspended floc dynamics in the Everglades and other environments with a near-logarithmic velocity profile and floc populations with comparable entrainment and settling relationships (i.e., most organic floc populations [Larsen *et al.*, 2009]), it is reasonable to adopt a single OFD that preserves fluxes downstream and to the bed.

[37] Use of an OFD in transport models disregards aggregation dynamics. Nevertheless, for many wetland floc transport models, disregarding aggregation dynamics will not introduce unacceptable error. On the rising limb of concentration curves, optimized aggregation parameters are not significantly different from zero for flow speeds below 7 cm s^{-1} . Aggregation is significant on the falling limb of the concentration curves, but the effects of enhanced settling to the bed via aggregation may be offset by hysteresis in entrainment rate that results in J_e values that are higher than expected. While disregarding aggregation-disaggregation dynamics in wetland floc transport models may only introduce small error, doing so in streams and other highly turbulent environments could produce unacceptable error in mass flux predictions [Wotton, 2007].

4.4. Implications for Floc Transport Through Vegetated Aquatic Environments

[38] Since bed shear stress in floodplains and wetlands is often near the critical bed shear stress for floc entrainment, spatial heterogeneity in shear stress as a result of microtopography and vegetation patchiness can lead to heterogeneity in floc erosion and deposition patterns, contributing to the topographic evolution of the wetland landscape and/or rates of nutrient cycling. In Everglades WCA-3A typical bed shear stresses lie orders of magnitude below the $1.0 \times 10^{-2} \text{ Pa}$ threshold for floc entrainment [Larsen *et al.*, 2009], so widespread bed floc entrainment events are rare in the present system. Instead, water column particle dynamics are most commonly characterized by low concentrations of small particles (mass- and volume-weighted mean diameters of 73 μm and 9 μm , respectively) dominated by local processes [Noe *et al.*, 2007]: biological production, bioturbation, and particle settling (Figure 1b). These fine particles have long immobilization times by single-particle settling [Larsen *et al.*, 2009] and are more reactive than the larger flocs, dominating phosphorus cycling in the water column [Noe *et al.*, 2003] and containing a higher nutrient density than larger flocs [Noe *et al.*, 2007]. Because of their reactivity and long residence times in the water column, fine particle transport alone may not contribute significantly to the topographic differentiation of the ridge and slough landscape. However, our annular flume experiments imply that differential settling is a significant process impacting Everglades floc. Given the larger mass per unit volume of fine particles [Larsen *et al.*, 2009] and their substantial contribution to total particle mass (section 4.2), incorpora-

tion of small particles into floc could significantly increase the magnitude of advective sediment and nutrient redistribution in the Everglades. Efficient interception of fine particles by periphyton and emergent vegetation stems, a process termed filtration (Figure 1), may serve as an additional mass redistribution process in the Everglades [Saiers *et al.*, 2003; Huang *et al.*, 2008] and other wetlands [Palmer *et al.*, 2004; D'Alpaos *et al.*, 2007].

[39] In contrast to typical conditions in the present-day Everglades, during transient high-flow events such as hurricanes or engineered releases of impounded water, water column particle dynamics would be dominated by the hydraulic processes of floc entrainment and transport. During these high flows bed shear stresses within sloughs could increase beyond the entrainment threshold, causing floc to become suspended. As in streams [Cushing *et al.*, 1993; Battin *et al.*, 2008], floc will be transported downstream in a series of distinct settling and reentrainment events. Reentrainment events are facilitated by hysteretic enhancement of J_e on the falling limb of the floc concentration curve (e.g., Table 3), which could result from disruption of the EPS that contributed to floc bed cohesion at the initiation of entrainment [Winterwerp and van Kesteren, 2004; Newbold *et al.*, 2005] or from the looser pore structure of the more recently deposited bed, permitting greater penetration of eddies that could generate lift.

[40] In most densely vegetated canopies, drag from macrophyte stems decreases flow velocities relative to open water areas [Kadlec, 1990; Nepf, 1999], promoting sedimentation [e.g., Furukawa *et al.*, 1997; Leonard and Reed, 2002; Pasternack and Brush, 2002]. Likewise, upon entering the dense emergent vegetation of ridges, flow carrying suspended floc from the sloughs will decrease in velocity, and the dominant vertical flux will become a settling flux (Figure 1a). This process is analogous to the deposition of floc on floodplains during periods of overbank flow [Nicholas and Walling, 1996]. Deposited flocs will undergo size sorting by distance. Assuming an OFD of 250 μm and negligible aggregation, the characteristic transport distance for suspended floc within the ridge at a mean water depth of 40 cm and mean water velocity of 1 cm s^{-1} would be approximately 10 m before settling to the bed occurred [Larsen *et al.*, 2009], which is consistent with a hypothesis of deposition in the vicinity of the ridge-slough transition [Larsen *et al.*, 2007]. Aggregation by differential settling within the ridge, particularly near the bed (Figure 4) will increase floc size and further decrease the characteristic transport distance for floc within the ridge. In contrast to sloughs, where hysteresis in J_e may compensate for aggregation-enhanced settling, in ridges the litter layer above the bed could shelter settling flocs from near-bed shear stresses or bind flocs in interstitial biofilm, resulting in permanent deposition.

[41] Two other studies within the greater Everglades that have characterized floc distribution and origin are consistent with the findings of this study. Using biochemical markers, Neto *et al.* [2006] found that (1) floc composition is largely detrital and related to local vegetation community composition and that (2) some decoupling in source-specific chemical markers between the floc and underlying peat implies limited hydrodynamic transport of floc, perhaps during episodic high-velocity events. While their study took

place along Taylor Slough, which has a marl substratum and floc with a larger inorganic (CaCO_3) content than floc from within the ridge and slough landscape, we expect these results to apply throughout the greater Everglades because of similar hydrodynamics and the relative ease of entraining floc with a high organic content. Similarly, using organic carbon quality as a tracer at site WCA-3A-5, Larsen [2008] found limited decoupling between the origin of surface peat and local vegetation community composition, which implies some allochthonous transport of organic material, possibly in the form of floc.

5. Conclusions

[42] In organoclastic slowly flowing environments where suspended particle concentrations are transport limited rather than supply limited, floc transport may dominate the surface water advective mass transfer of carbon and nutrients and contribute to the evolution of microtopography. Downstream transport of floc in areas where bed shear stress exceeds the entrainment threshold will be characterized by multiple deposition and reentrainment events, facilitated by the higher entrainment flux of recently deposited floc beds relative to more established beds. In regions where settling is the dominant flux, aggregation of floc by differential settling further enhances sedimentation, while at the highest flow speeds, aggregation occurs as a result of particle-particle collisions but competes with disaggregation. However, over a range of typical flow velocities for inland wetlands and floodplains, floc aggregation processes dominate over disaggregation. Differences in flow velocities and shear stresses within different vegetation communities may result in the transfer of organic matter and nutrients from relatively open areas to more densely vegetated parts of the aquatic ecosystem.

[43] Floc dynamics within wetlands, floodplains, and shallow streams are complex because of a wide range of floc sizes, hysteresis in entrainment rates and fractal dimension, differences in microbial communities and the organic character of floc, diel patterns of biological activity, and multiple mechanisms of particle aggregation. During periods when bed shear stresses are below the floc entrainment threshold, biological processes such as bioturbation and new particle production are dominantly responsible for water column floc dynamics. Nightly occurring thermal overturn, in contrast, does not cause significant floc entrainment in the Everglades. Despite the complexity of floc dynamics in shallow, slowly flowing environments, when mean flow controls water column floc dynamics (i.e., when bed shear stresses are above the floc entrainment threshold), it is viable to predict the essential dynamics of floc transport through simplified numerical modeling. The proposed modeling scheme tracks the balance between entrainment, settling, and advective transport for multiple size classes or for a single size class using an OFD that results in a correct settling flux to the bed while minimizing error in the vertically averaged concentration of floc transported downstream. Models can ignore floc aggregation dynamics with minimal error at flows associated with bed shear stresses just above the floc entrainment threshold, but at the highest flows (e.g., 7.0 cm s^{-1} in the annular flume experiments) or at moderate flows that follow periods of high flow, aggre-

gation becomes significant and models should simulate multiple size classes.

[44] Water management decisions in the Everglades would need to define a target flow velocity that optimizes the transfer of organic sediment from sloughs to ridges. On the basis of our experiments and conceptual model, a target velocity should result in shear stresses above the 1.0×10^{-2} Pa entrainment threshold in sloughs and just below the entrainment threshold within ridges. Simulations of differential flow velocities and shear stresses through heterogeneous vegetation communities under different combinations of water depths and energy slopes would provide the remaining piece of information needed to propose target velocities and durations of elevated flow that are most likely to sustain an Everglades that redistributes suspended floc in ways that maintain landscape structure and biodiversity.

[45] **Acknowledgments.** We thank Daniel Nowacki for field and analytical assistance and Kevin Brett for image processing work. Charlotte Fuller provided access to the flumes at the Rutgers IMCS seawater lab and generous laboratory assistance. This work was funded by NSF award EAR-0636079, the USGS Priority Ecosystems Studies Program, the USGS National Research Program, the Canon National Parks Science Scholars Program, an NSF graduate research fellowship to LGL, and a Hertz Foundation fellowship to LGL. This manuscript benefited from the helpful reviews of Jeffrey King, Jonathan Nelson, Roger Wotton, and two anonymous reviewers. Any use of trade, firm, or product names is for descriptive purposes only and does not imply endorsement by the U.S. government.

References

- Allredge, A. L., and C. Gotschalk (1988), In situ settling behavior of marine snow, *Limnol. Oceanogr.*, **33**, 339–351.
- Battin, T. J., L. A. Kaplan, S. Findlay, C. S. Hopkins, E. Marti, A. I. Packman, J. D. Newbold, and F. Sabater (2008), Biophysical controls on organic carbon fluxes in fluvial networks, *Nat. Geosci.*, **1**, 95–100, doi:10.1038/ngeo101.
- Bernhardt, C. E., D. A. Willard, M. Marot, and C. W. Holmes (2004), Anthropogenic and natural variation in ridge and slough pollen assemblages, *U.S. Geol. Surv. Open File Rep.*, 2004-1448, 47 pp.
- Burban, P. Y., W. Lick, and J. Lick (1989), The flocculation of fine-grained sediments in estuarine waters, *J. Geophys. Res.*, **94**, 8323–8330, doi:10.1029/JC094iC06p08323.
- Chen, S., and D. Eisma (1995), Fractal geometry of in situ flocs in the estuarine and coastal environments, *Neth. J. Sea Res.*, **33**, 173–182, doi:10.1016/0077-7579(95)90004-7.
- Christiansen, T., P. L. Wiberg, and T. G. Milligan (2000), Flow and sediment transport on a tidal salt marsh surface, *Estuarine Coastal Shelf Sci.*, **50**, 315–331, doi:10.1006/ecs.2000.0548.
- Cushing, C. E., G. W. Minshall, and J. D. Newbold (1993), Transport dynamics of fine particulate organic matter in two Idaho streams, *Limnol. Oceanogr.*, **38**, 1101–1115.
- D'Alpaos, A., S. Lanzoni, M. Marani, and A. Rinaldo (2007), Landscape evolution in tidal embayments: Modeling the interplay of erosion, sedimentation, and vegetation dynamics, *J. Geophys. Res.*, **112**, F01008, doi:10.1029/2006JF000537.
- de Boer, D. H. (1997), An evaluation of fractal dimensions to quantify changes in the morphology of fluvial suspended sediment particles during baseflow conditions, *Hydrol. Processes*, **11**, 415–426, doi:10.1002/(SICI)1099-1085(19970330)11:4<415::AID-HYP450>3.0.CO;2-W.
- Droppo, I. G. (2003), A new definition of suspended sediment: Implications for the measurement and prediction of sediment transport, in *Erosion and Sediment Transport Measurement in Rivers: Technological and Methodological Advances*, edited by J. Bogen, T. Fergus, and D. E. Walling, *IAHS Publ.*, **283**, 3–12.
- Droppo, I. G. (2004), Structural controls on floc strength and transport, *Can. J. Civ. Eng.*, **31**, 569–578, doi:10.1139/04-015.
- Droppo, I. G., Y. L. Lau, and C. Mitchell (2001), The effect of depositional history on contaminated bed sediment stability, *Sci. Total Environ.*, **266**, 7–13, doi:10.1016/S0048-9697(00)00748-8.
- Dyer, K. R., and A. J. Manning (1999), Observation of the size, settling velocity and effective density of flocs, and their fractal dimensions, *J. Sea Res.*, **41**, 87–95, doi:10.1016/S1385-1101(98)00036-7.
- Eisma, D., T. Schuhmacher, H. Boekel, J. VanHeerwaarden, H. Franken, M. Laan, A. Vaars, F. Eijgenraam, and J. Kalf (1990), A camera and image-analysis system for in situ observation of flocs in natural waters, *Neth. J. Sea Res.*, **27**, 43–56, doi:10.1016/0077-7579(90)90033-D.
- Furukawa, K., E. Wolanski, and H. Mueller (1997), Currents and sediment transport in mangrove forests, *Estuarine Coastal Shelf Sci.*, **44**, 301–310, doi:10.1006/ecs.1996.0120.
- Grant, J., and G. Gust (1987), Prediction of coastal sediment stability from photopigment content of mats of purple sulphur bacteria, *Nature*, **330**, 244–246, doi:10.1038/330244a0.
- Gunderson, L. H. (1994), Vegetation of the Everglades: Determinants of community composition, in *Everglades: The Ecosystem and Its Restoration*, edited by S. M. Davis and J. C. Ogden, pp. 323–340, St. Lucie, Delray Beach, Fla.
- Gunderson, L. H., and W. F. Loftus (1993), The Everglades, in *Biodiversity of the Southeastern United States: Terrestrial Communities*, edited by W. H. Martin, S. G. Boyce, and A. C. Echternacht, chap. 6, pp. 199–256, John Wiley, New York.
- Harvey, J. W., J. E. Saiers, and J. T. Newlin (2005), Solute transport and storage mechanisms in wetlands of the Everglades, south Florida, *Water Resour. Res.*, **41**, W05009, doi:10.1029/2004WR003507.
- Harvey, J. W., R. W. Schaffranek, L. G. Larsen, D. Nowacki, G. B. Noe, and B. L. O'Connor (2008), Controls on flow velocity and flow resistance in the patterned floodplain landscape of the Everglades, paper presented at Ocean Sciences Meeting, Am. Soc. of Limnol. and Oceanogr., Orlando, Fla., 2–7 March.
- Hill, P. S., G. Voulgaris, and J. H. Trowbridge (2001), Controls on floc size in a continental shelf bottom boundary layer, *J. Geophys. Res.*, **106**, 9543–9549, doi:10.1029/2000JC900102.
- Huang, H. (1994), Fractal properties of flocs formed by fluid shear and differential settling, *Phys. Fluids*, **6**, 3229–3234, doi:10.1063/1.868055.
- Huang, Y. H., J. E. Saiers, J. W. Harvey, G. B. Noe, and S. Mylon (2008), Advection, dispersion, and filtration of fine particles within emergent vegetation of the Florida Everglades, *Water Resour. Res.*, **44**, W04408, doi:10.1029/2007WR006290.
- Kadlec, R. H. (1990), Overland flow in wetlands-vegetation resistance, *J. Hydraul. Eng.*, **116**, 691–706, doi:10.1061/(ASCE)0733-9429(1990)116:5(691).
- Krishnappan, B. G. (1991), A rotating flume for cohesive sediment transport research, *Contrib. 91-82*, Natl. Water Res. Inst., Burlington, Ont., Canada.
- Krishnappan, B. G. (1993), Rotating circular flume, *J. Hydraul. Eng.*, **119**, 758–767, doi:10.1061/(ASCE)0733-9429(1993)119:6(758).
- Larsen, L. G. (2008), Hydroecological feedback processes governing self-organization of the Everglades ridge and slough landscape, Ph.D. thesis, Univ. of Colo., Boulder.
- Larsen, L. G., J. W. Harvey, and J. P. Crimaldi (2007), A delicate balance: Ecohydrological feedbacks governing landscape morphology in a lotic peatland, *Ecol. Monogr.*, **77**, 591–614, doi:10.1890/06-1267.1.
- Larsen, L. G., J. W. Harvey, and J. P. Crimaldi (2009), Morphologic, settling, and entrainment characteristics of organic wetland floc, Everglades, Florida, doi:10.1029/2008WR006990, in press.
- Lau, Y. L., I. G. Droppo, and B. G. Krishnappan (2001), Sequential erosion/deposition experiments—Demonstrating the effects of depositional history on sediment erosion, *Water Res.*, **35**, 2767–2773, doi:10.1016/S0043-1354(00)00559-5.
- Leonard, L. A., and M. E. Luther (1995), Flow hydrodynamics in tidal marsh canopies, *Limnol. Oceanogr.*, **40**, 1474–1484.
- Leonard, L. A., and D. J. Reed (2002), Hydrodynamics and sediment transport through tidal marsh canopies, *J. Coastal Res.*, **36**, 459–469.
- Lick, W., J. Lick, and K. Ziegler (1992), Flocculation and its effect on the vertical transport of fine-grained sediments, *Hydrobiologia*, **235–236**, 1–16, doi:10.1007/BF00026196.
- Lodge, T. (1994), *The Everglades Handbook: Understanding the Ecosystem*, St. Lucie, Delray Beach, Fla.
- Logan, B. E., and D. B. Wilkinson (1990), Fractal geometry of marine snow and other biological aggregates, *Limnol. Oceanogr.*, **35**, 130–136.
- Masson, S., B. Pinel-Alloul, and P. Dutilleul (2004), Spatial heterogeneity of zooplankton biomass and size structure in southern Quebec lakes: Variation among lakes and within lake among epi-, meta- and hypolimnion strata, *J. Plankton Res.*, **26**, 1441–1458, doi:10.1093/plankt/fbh138.
- Mayer, L. M., L. L. Schick, K. Skorko, and E. Boss (2006), Photodissolution of particulate organic matter from sediments, *Limnol. Oceanogr.*, **51**, 1064–1071.
- Mehta, A. J., and E. Partheniades (1975), An investigation of the depositional properties of flocculated fine sediments, *J. Hydraul. Res.*, **13**, 361–381.

- Middleton, G. V., and J. B. Southard (1984), *Mechanics of Sediment Movement, SEPM Short Course 3*, Soc. for Sediment. Geol., Tulsa, Okla.
- National Research Council (2003), *Does Water Flow Influence Everglades Landscape Patterns?*, 41 pp., Natl. Acad., Washington, D. C.
- Nepf, H. M. (1999), Drag, turbulence, and diffusion in flow through emergent vegetation, *Water Resour. Res.*, *35*, 479–489, doi:10.1029/1998WR900069.
- Neto, R. R., R. N. Mead, J. W. Louda, and R. Jaffe (2006), Organic biogeochemistry of detrital flocculent material (floc) in a subtropical, coastal wetland, *Biogeochemistry*, *77*, 283–304, doi:10.1007/s10533-005-5042-1.
- Newbold, J. D., S. A. Thomas, G. W. Minshall, C. E. Cushing, and T. Georgian (2005), Deposition, benthic residence, and resuspension of fine organic particles in a mountain stream, *Limnol. Oceanogr.*, *50*, 1571–1580.
- Nezu, I., and H. Nakagawa (1993), *Turbulence in Open-Channel Flows*, A.A. Balkema, Rotterdam, Netherlands.
- Nicholas, A. P., and D. E. Walling (1996), The significance of particle aggregation in the overbank deposition of suspended sediment on river floodplains, *J. Hydrol.*, *186*, 275–293, doi:10.1016/S0022-1694(96)03023-5.
- Noe, G. B., L. J. Scinto, J. Taylor, D. L. Childers, and R. D. Jones (2003), Phosphorus cycling and partitioning in an oligotrophic Everglades wetland ecosystem: A radioisotope tracing study, *Freshwater Biol.*, *48*, 1993–2008, doi:10.1046/j.1365-2427.2003.01143.x.
- Noe, G. B., J. Harvey, and J. Saiers (2007), Characterization of suspended particles in Everglades wetlands, *Limnol. Oceanogr.*, *52*, 1166–1178.
- Noe, G. B., J. W. Harvey, and L. G. Larsen (2008), Biogeochemical transformations and transport related to flow in the ridge and slough landscape, paper presented at Greater Everglades Ecosystem Restoration Conference, U.S. Geol. Surv., Naples, Fla., 28 July to 1 Aug.
- Ogden, J. C. (2005), Everglades ridge and slough conceptual ecological model, *Wetlands*, *25*, 810–820, doi:10.1672/0277-5212(2005)025[0810:ERASCE]2.0.CO;2.
- Palmer, M. R., H. M. Nepf, T. J. R. Pettersson, and J. D. Ackerman (2004), Observations of particle capture on a cylindrical collector: Implications for particle accumulation and removal in aquatic systems, *Limnol. Oceanogr.*, *49*, 76–85.
- Partheniades, E. (1977), Unified view of wash load and bed material load, *J. Hydraul. Div. Am. Soc. Civ. Eng.*, *103*, 1037–1057.
- Pasternack, G. B., and G. S. Brush (2002), Biogeomorphic controls on sedimentation and substrate on a vegetated tidal freshwater delta in upper Chesapeake Bay, *Geomorphology*, *43*, 293–311, doi:10.1016/S0169-555X(01)00139-8.
- Petersen, O., and B. G. Krishnappan (1994), Measurement and analysis of flow characteristics in a rotating circular flume, *J. Hydraul. Res.*, *32*, 483–494.
- Saiers, J. E., J. W. Harvey, and S. E. Mylon (2003), Surface-water transport of suspended matter through wetland vegetation of the Florida everglades, *Geophys. Res. Lett.*, *30*(19), 1987, doi:10.1029/2003GL018132.
- Schaffranek, R. W., and H. L. Jenter (2001), Observations of daily temperature patterns in the southern Florida Everglades, paper presented at Wetlands Engineering and River Restoration Conference, Am. Soc. of Civ. Eng., Reno, Nev., 27–31 Aug.
- Spicer, P. T., and S. E. Pratsinis (1996), Shear-induced flocculation: The evolution of floc structure and the shape of the size distribution at steady state, *Water Res.*, *30*, 1049–1056, doi:10.1016/0043-1354(95)00253-7.
- Sterling, M. C., Jr., J. S. Bonner, A. N. S. Ernest, C. A. Page, and R. L. Autenrieth (2005), Application of fractal flocculation and vertical transport model to aquatic soil-sediment systems, *Water Res.*, *39*, 1818–1830, doi:10.1016/j.watres.2005.02.007.
- Stone, M., and B. G. Krishnappan (2003), Floc morphology and size distributions of cohesive sediment in steady-state flow, *Water Res.*, *37*, 2739–2747, doi:10.1016/S0043-1354(03)00082-4.
- Thomas, D. N., S. J. Judd, and N. Fawcett (1999), Flocculation modelling: A review, *Water Res.*, *33*, 1579–1592, doi:10.1016/S0043-1354(98)00392-3.
- U.S. Army Corps of Engineers (1999), Central and southern Florida project, Comprehensive review study, final integrated feasibility report and programmatic environmental impact statement, Washington, D. C.
- Walling, D. E., and P. W. Moorehead (1989), The particle size characteristics of fluvial suspended sediment: An overview, *Hydrobiologia*, *176–179*, 125–149, doi:10.1007/BF00026549.
- Willard, D. A., L. M. Weimer, and W. L. Riegel (2001), Pollen assemblages as paleoenvironmental proxies in the Florida Everglades, *Rev. Palaeobot. Palynol.*, *113*, 213–235, doi:10.1016/S0034-6667(00)00042-7.
- Winterwerp, J. C., and W. G. M. van Kesteren (2004), *Introduction to the Physics of Cohesive Sediment in the Marine Environment*, Elsevier, Amsterdam.
- Wotton, R. S. (2007), Do benthic biologists pay enough attention to aggregates formed in the water column of streams and rivers?, *J.N. Am. Benthol. Soc.*, *26*, 1–11, doi:10.1899/0887-3593(2007)26[1:DBBPEA]2.0.CO;2.
- Wu, Y., N. Wang, and K. Rutchey (2006), An analysis of spatial complexity of ridge and slough patterns in the Everglades ecosystem, *Ecol. Complexity*, *3*, 183–192, doi:10.1016/j.ecocom.2005.12.002.

J. P. Crimaldi, Department of Civil, Environmental, and Architectural Engineering, University of Colorado, 428 UCB, Boulder, CO 80309, USA.

J. W. Harvey, L. G. Larsen, and G. B. Noe, U.S. Geological Survey, 430 National Center, Reston, VA 20192, USA. (lglarsen@usgs.gov)